Heat Mass Transfer (2008) 44:727–737
DOI 10.1007/s00231-007-0301-4

ORIGINAL

Simulation studies on multi-mode heat transfer from an open cavity with a flush-mounted discrete heat source

C. Gururaja Rao · V. Nagabhushana Rao · C. Krishna Das

Received: 10 January 2007 / Accepted: 5 June 2007 / Published online: 14 July 2007
© Springer-Verlag 2007

Abstract Prominent results of a simulation study on conjugate convection with surface radiation from an open cavity with a traversable flush mounted discrete heat source in the left wall are presented in this paper. The open cavity is considered to be of fixed height but with varying spacing between the legs. The position of the heat source is varied along the left leg of the cavity. The governing equations for temperature distribution along the cavity are obtained by making energy balance between heat generated, conducted, convected and radiated. Radiation terms are tackled using radiosity-irradiation formulation, while the view factors, therein, are evaluated using the crossed-string method of Hottel. The resulting non-linear partial differential equations are converted into algebraic form using finite difference formulation and are subsequently solved by Gauss–Seidel iterative technique. An optimum grid system comprising 111 grids along the legs of the cavity, with 30 grids in the heat source and 31 grids across the cavity has been used. The effects of various parameters, such as surface emissivity, convection heat transfer coefficient, aspect ratio and thermal conductivity on the important results, including local temperature distribution along the cavity, peak temperature in the left and right legs of the cavity and relative contributions of convection and radiation to heat dissipation in the cavity, are studied in great detail.

C. Gururaja Rao (✉) · V. Nagabhushana Rao · C. Krishna Das
Department of Mechanical Engineering,
National Institute of Technology,
[Formerly, Regional Engineering College Warangal],
Warangal 506 004, AP, India
e-mail: cgr_gcr@yahoo.co.in

List of symbols

A	aspect ratio
F_{ik}	view factor of an element i with reference to another element k of the cavity
h	convection heat transfer coefficient (W/m^2 K)
$J(i, j)$	radiosity of an element (i, j) of the enclosure (W/m^2)
k	thermal conductivity of the cavity walls and heat source (W/m K)
L	height of open cavity (m)
L_1	distance between bottom end of the cavity and the start of heat source (m)
L_h	height of the discrete heat source (m)
M	total number of grids along the leg
M_1	total number of grids between bottom end of the cavity and the start of heat source
M_2	total number of grids between bottom end of the cavity and the end of heat source
N	total number of grids across the cavity
n'	total number of elements in the cavity
Pr	Prandtl number of air
q_v	volumetric heat generation in the heat source (W/m^3)
S	spacing between the legs of the cavity (m)
t	thickness of each wall of the cavity (m)
T	temperature at any location in the cavity (K or °C)
T_{max}	maximum temperature in the cavity (K or °C)
T_∞	ambient air temperature (K or °C)
x	co-ordinate direction along the cavity
y	co-ordinate direction across the cavity

Greek symbols

δ_c	convergence criterion, in percentage, $\left\lvert (T_{new} - T_{old})/T_{new} \right\rvert \times 100\%$

Δx height of the wall element in non-heat source portion along the cavity (m)
Δx_h height of the wall element in heat source portion (m)
Δy height of the wall element in non-heat source portion across the cavity (m)
ε surface emissivity of the walls of the cavity
σ Stefan–Boltzmann constant (5.6697×10^{-8} W/m^2 K^4)

Subscripts

cond, x, in conduction heat transfer into an element along the cavity
cond, x, out conduction heat transfer out of an element along the cavity
cond, y, in conduction heat transfer into an element across the cavity
cond, y, out conduction heat transfer out of an element across the cavity
conv convection heat transfer from an element
conv, horz convection heat transfer from the horizontal surface of the unique element
conv, vert convection heat transfer from the vertical surface of the unique element
gen volumetric heat generation in an element
i any arbitrary element along the cavity
j any arbitrary element across the cavity
new, old temperatures from current and previous iterations, respectively
rad heat transfer by surface radiation from an element
rad, horz radiation heat transfer from the horizontal surface of the unique element
rad, vert radiation heat transfer from the vertical surface of the unique element

1 Introduction

Starting probably with the work of Zinnes [1], which dates back to the year 1970, studies on problems involving multiple modes of heat transfer continue to find place in the literature. To briefly elaborate some such works, Anand et al. [2] probed the effect of wall conduction on natural convection between asymmetrically heated isothermal vertical flat plates. Tewari and Jaluria [3] studied mixed convection heat transfer from horizontal and vertical plates mounted with thermal sources. Merkin and Pop [4] analyzed the problem of conjugate natural convection from a vertical surface. Dehghan and Behnia [5] made a thorough study on combined natural convection, conduction and radiation from an open cavity provided with discrete heating along the left wall. Cole [6] has presented his results of the problem of conjugate heat transfer from a small heated strip. Gururaja Rao et al. [7] have provided the results of conjugate mixed convection with surface radiation from a vertical plate provided with a flush-mounted discrete heat source. They deviated from the conventional studies reported in the literature, in which the boundary layer approximations were used, and solved the above problem considering the Navier–Stokes equations in their full strength. Gururaja Rao et al. [8, 9] have also made multimode heat transfer studies, comprising mixed convection, conduction and radiation, for the geometry of vertical channel with, respectively, symmetric and uniform wall heat generation and flush-mounted discrete heat sources in each of the walls. Gururaja Rao [10] probed the problem of buoyancy-aided mixed convection with conduction and surface radiation from a vertical electronic board provided with a traversable discrete heat source. Here, he studied the effect of changing the position of the heat source along the board on various results concerning the problem, including peak board temperature, local board temperature distribution and relative contributions of convection and radiation in heat dissipation. Gururaja Rao et al. [11] have very recently presented the results of simulation studies on multimode heat transfer from a square shaped electronic device with multiple discrete heat sources.

A thorough look at the literature pertaining to multimode heat transfer, some of the details of which are enunciated above, reveals that not much information is available on interaction of radiation with conjugate convection from a discretely heated open cavity taking into account (i) changing heat source position and (ii) changing cavity wall spacing. In view of the above, in the present paper, an attempt is made to numerically investigate conduction–convection–radiation heat transfer in an open cavity that is provided with a flush-mounted discrete heat source in its left wall. The study not only takes into account the varying heat source position along the left limb of the cavity but also looks into the effect of varying the spacing between the two walls of the cavity.

2 Mathematical formulation

The schematic of the geometry chosen for the present problem is shown in Fig. 1. It consists of an open cavity of height L and spacing S. The thickness of the wall (or leg) of the cavity is t, while the thermal conductivity of the material, the cavity is composed of, is k. There is a flush-mounted discrete heat source of height L_h and thickness t provided in the left wall of the cavity. It is possible to traverse the heat source along the left leg of the cavity such that the heat source can take up any position starting from entry of the cavity to the bottommost position in the cavity. L_1 is the

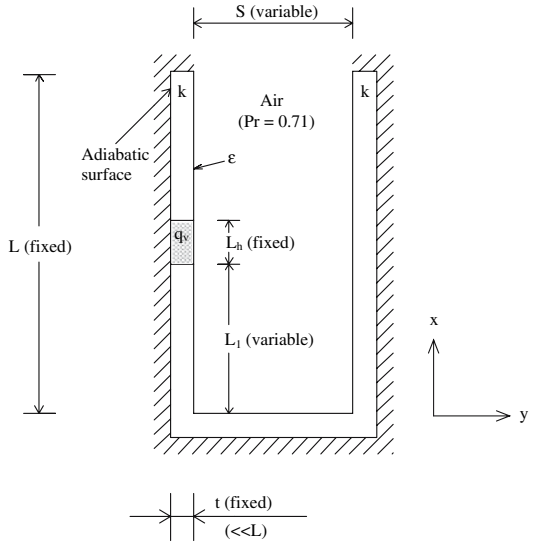

Fig. 1 Schematic of the problem geometry chosen for study

distance between the bottom of the cavity and the start of the heat source. Thus, L_1 can take up any value starting from 0 to $L - L_h$. The surface emissivity of the cavity is ε and the cavity is dissipating heat to the cooling agent (air) at a temperature T_∞ with h as the pertinent convection heat transfer coefficient. An aspect ratio (A) is defined as L/S, and its value can be varied, which offers different possibilities starting from a narrow cavity to a broadly spaced cavity. The cavity is considered to be adiabatic on its entire outer surface including the two top ends of the legs of the cavity. This implies heat dissipation occurring only from the inner surfaces of the cavity to the ambient air. The thickness of the wall of the cavity is much smaller than the height, thus rendering heat conduction in the cavity walls one-dimensional. The coordinate direction x is chosen along the cavity, while y is considered across the cavity.

In order to get the temperature distribution in the entire cavity, it would be required to make energy balance between the heat generated, the heat conducted, the heat convected and the heat radiated. In order to tackle the radiation related terms in the above calculation, radiosity-irradiation formulation would be employed, while for obtaining the view factors therein, the Hottel's crossed-string method is employed.

For obtaining the governing equation for temperature distribution in the heat source portion of the left leg of the cavity (other than the end points of the heat source), making energy balance on an element results in

$$q_{\text{cond},x,\text{in}} + q_{\text{gen}} = q_{\text{cond},x,\text{out}} + q_{\text{conv}} + q_{\text{rad}} \tag{1}$$

By making substitution for different terms in the above equation and simplifying, one gets

$$\begin{aligned} q_v \Delta x_h t = {} & -kt \frac{\partial^2 T(i,1)}{\partial x^2} \Delta x_h + h \Delta x_h [T(i,1) - T_\infty] \\ & + \frac{\varepsilon}{1-\varepsilon} \left[\sigma T^4(i,1) - J(i,1)\right] \Delta x_h \end{aligned} \tag{2}$$

where $J(i,1) = \varepsilon \sigma T^4(i,1) + (1-\varepsilon) \sum_{k=1}^{n'} F_{ik} J_k$.

Here, n' stands for the total number of elements in the enclosure encompassing the three solid boundaries, namely the left and right legs of the cavity and its bottom surface plus the top free boundary of the cavity.

Since the heat source can move from the bottommost to the topmost ends of the left leg of the cavity, its interfaces with the left leg would have different equations governing the variation of their temperatures. For example, if the heat source is somewhere in between the top and bottommost ends of the left leg, then, making energy balance for the element pertaining to the bottom end of the heat source,

$$q_{\text{cond},x,\text{in}} + q_{\text{gen}} = q_{\text{cond},x,\text{out}} + q_{\text{conv}} + q_{\text{rad}} \tag{3}$$

The above equation, after appropriate simplification, leads to

$$\begin{aligned} q_v \frac{\Delta x_h}{2} t = {} & -kt \frac{\partial^2 T(i,1)}{\partial x^2} \frac{(\Delta x + \Delta x_h)}{2} \\ & + h \frac{(\Delta x + \Delta x_h)}{2} [T(i,1) - T_\infty] \\ & + \frac{\varepsilon}{1-\varepsilon} \left[\sigma T^4(i,1) - J(i,1)\right] \frac{(\Delta x + \Delta x_h)}{2} \end{aligned} \tag{4}$$

The governing equation for the top end of the heat source is also obtained using similar treatment. The temperature at any point in the non-heat source portion of the left leg of the cavity is governed by the relation:

$$q_{\text{cond},x,\text{in}} = q_{\text{cond},x,\text{out}} + q_{\text{conv}} + q_{\text{rad}} \tag{5}$$

The above equation, upon simplification, gives rise to

$$\begin{aligned} & kt \frac{\partial^2 T(i,1)}{\partial x^2} \Delta x - h \Delta x [T(i,1) - T_\infty] \\ & - \frac{\varepsilon}{1-\varepsilon} \left[\sigma T^4(i,1) - J(i,1)\right] \Delta x = 0 \end{aligned} \tag{6}$$

It is to be noted that in the equations hitherto or anywhere else hereafter, Δx pertains to the length of the appropriate element. For the top adiabatic end of the left leg of the cavity, the energy balance gives

$$q_{\text{cond},x,\text{in}} = q_{\text{conv}} + q_{\text{rad}} \tag{7}$$

After simplification, the above equation modifies to

$$kt\frac{\partial T(i,1)}{\partial x} - h\frac{\Delta x}{2}[T(i,1) - T_\infty] - \frac{\varepsilon}{1-\varepsilon}\left[\sigma T^4(i,1) - J(i,1)\right]\frac{\Delta x}{2} = 0 \tag{8}$$

The temperature of the left bottom corner of the cavity is obtained by making energy balance as

$$q_{\text{cond},x,\text{out}} + q_{\text{cond},y,\text{out}} + q_{\text{conv,vert}} + q_{\text{conv,horz}} + q_{\text{rad,vert}} + q_{\text{rad,horz}} = 0 \tag{9}$$

Appropriate simplification of the above equation would lead to

$$kt\frac{\partial T(i,1)}{\partial x} + kt\frac{\partial T(1,j)}{\partial y} - h\frac{\Delta x}{2}[T(i,1) - T_\infty] - h\frac{\Delta y}{2}[T(1,j) - T_\infty] - \frac{\varepsilon}{1-\varepsilon}\left[\sigma T^4(i,1) - J_1(i,1)\right]\frac{\Delta x}{2} - \frac{\varepsilon}{1-\varepsilon}\left[\sigma T^4(1,j) - J_2(1,j)\right]\frac{\Delta y}{2} = 0 \tag{10}$$

Here $J_1(i,1)$ and $J_2(1,j)$ are the radiosities of the left leg and the bottom surface portions of the corresponding element. With regard to the right wall of the cavity, which does not contain any heat source, the energy balance on a given element, other than the bottommost and the topmost points of the wall, gives

$$q_{\text{cond},x,\text{in}} = q_{\text{cond},x,\text{out}} + q_{\text{conv}} + q_{\text{rad}} \tag{11}$$

The above equation, in its modified form, will be

$$kt\frac{\partial^2 T(i,N)}{\partial x^2}\Delta x - h\Delta x[T(i,N) - T_\infty] - \frac{\varepsilon}{1-\varepsilon}\left[\sigma T^4(i,N) - J(i,N)\right]\Delta x = 0 \tag{12}$$

The governing equations for the temperatures of the bottom right corner of the cavity and the top adiabatic end of the right leg are also obtained appropriately using similar treatment. Likewise, the surface joining the two legs of the cavity too does not possess any heat source. Its temperature distribution obeys the following energy balance equation:

$$q_{\text{cond},y,\text{in}} = q_{\text{cond},y,\text{out}} + q_{\text{conv}} + q_{\text{rad}} \tag{13}$$

The above equation takes up the following form after its simplification:

$$kt\frac{\partial^2 T(1,j)}{\partial y^2}\Delta y - h\Delta y[T(1,j) - T_\infty] - \frac{\varepsilon}{1-\varepsilon}\left[\sigma T^4(1,j) - J(1,j)\right]\Delta y = 0 \tag{14}$$

Finally, the free or open boundary of the computational domain pertaining to the open end of the cavity is assumed to be isothermal and at the temperature of that of air (T_∞). Further, its surface is assumed black with an emissivity equal to unity.

3 Method of solution and range of parameters

The governing equations for temperature distribution in the entire computational domain obtained in the preceding section are non-linear partial differential equations. As a first step to solving them, the above equations are transformed into algebraic form using finite difference method. The algebraic equations thus obtained are subsequently solved using Gauss–Seidel iterative technique. Full relaxation (relaxation parameter = 1) is imposed on temperature with a stringent convergence criterion (δ_c) equal to 10^{-8} used for terminating iterations.

The height (L) of the cavity is fixed at 20 cm, while the wall thickness of the cavity (t) is always taken to be 1.5 mm. The height of the discrete heat source (L_h) is equal to $L/8$ (2.5 cm). Since the heat source is flush-mounted, its thickness (t) is the same as that of the cavity wall, i.e., 1.5 mm. The cooling medium (air) is considered to be at a temperature (T_∞) of 25°C. The ranges of different other parameters needed in the study are fixed after some initial studies. The aspect ratio (A) is varied between 0.5 and 20, thus simulating a widely spaced cavity to a narrow cavity. The volumetric heat generation (q_v) would take up any value between 10^5 and 10^6 W/m^3, though most of the studies in the present work are made for $q_v = 10^6$ W/m^3 owing to the fact that it gives the highest of the temperatures and its control would be the point of interest for the designer. The surface emissivity (ε) is varied between 0.05 and 0.85 for the reason that good reflectors and good emitters, respectively, typically have the above values of emissivity. The range for convection heat transfer coefficient (h) is considered to be 5–100 W/m^2 K. The above is done since the asymptotic free and forced convection limits with gaseous cooling agents would generally be 5 and 100 W/m^2 K. With regard to thermal conductivity (k), the values are varied between 0.25 and 1 W/m K since electronic devices typically have k of the order of unity.

4 Results and discussion

Before carrying out a parametric study pertaining to the present problem, the optimum grid system needed for discretisation of the computational domain is arrived at based on an exhaustive grid sensitivity analysis (Fig. 2).

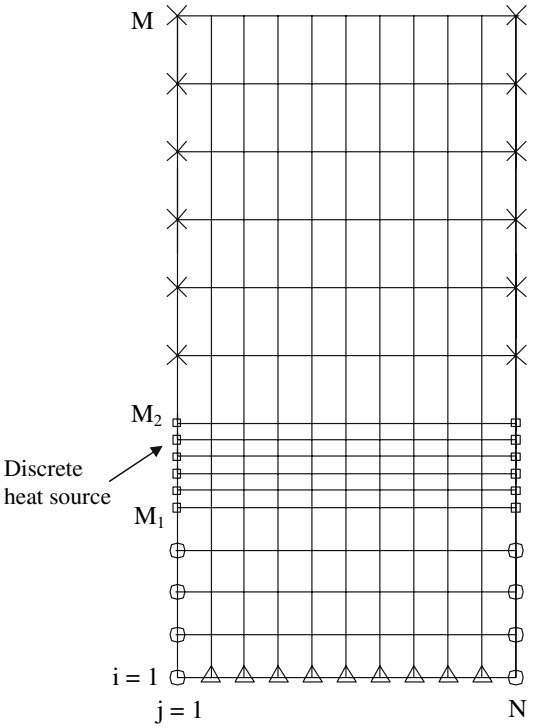

Fig. 2 Representative diagram showing the grid system considered for any arbitrary position of the heat source

4.1 Grid sensitivity analysis

In the present work, the discrete heat source in the left leg (or wall) of the open cavity is traversed from the bottom of the cavity to the top with five typical positions chosen. They are bottommost position, central position, topmost position and two more positions midway between the above three positions. The grid study is performed for a fixed set of parameters, viz., $q_v = 10^6$ W/m^3, $k = 0.25$ W/m K, $h = 5$ W/m^2 K, $\varepsilon = 0.45$ and $A = 12$. In the first stage of the above study (Tables 1, 2, 3), the heat source is at the bottommost position implying $L_1 = 0$, while the total number of grids along the leg (M) is taken to be 111, and across the cavity (N) is taken to be 51. Obviously, here $M_1 = 1$. The number of grids along the heat source ($M_2 - M_1$) is varied. The results from the Table 1 indicate that the maximum temperature (T_{max}) changes by 0.91% as ($M_2 - M_1$) increases from 10 to 20, while a further increase of ($M_2 - M_1$) to 30 brings down the change in T_{max} to 0.71%. An increase in ($M_2 - M_1$) beyond 30 showed an increase in the change in T_{max} too. In view of this, ($M_2 - M_1$) is fixed at 30. Table 1 shows a satisfactory energy balance check also for the above value of ($M_2 - M_1$). Keeping ($M_2 - M_1$) = 30 and all other parameters same as above, the total number of grids along the leg of the cavity (M) is varied and the results can be seen in Table 2. The table shows that T_{max} changes by only 0.17% as M is increased from 111 to 121. Thus the value of M is fixed to be 111. Subsequently keeping $M = 111$, ($M_2 - M_1$) = 30 and the rest of the parameters as above, the number of grids across the cavity (N) is varied. The results obtained are shown in Table 3, which shows only 0.08% change in T_{max} as N increases from 21 to 31.

In the second stage of grid study, the heat source takes position midway between the bottommost and the central positions along the leg. Here, for ($M_2 - M_1$) = 30 and rest of the parameters as in stage 1, results are obtained by varying: (i) firstly M_1 with $M = 91$ and $N = 21$, (ii) secondly M with $M_1 = 41$ and $N = 21$ and (iii) subsequently

Table 1 Heat source at the bottom end of the cavity $M = 111$, $N = 51$ and $M_1 = 1$ ($A = 12$, $\varepsilon = 0.45$, $h = 5$ W/m^2 K, $k = 0.25$ W/m K)

S. no.	$M_2 - M_1$	T_{max} (°C)	Percentage change (abs.)	Discrepancy in energy balance (%)
1	10	160.4674	–	1.258
2	20	161.9295	0.911	0.458
3	30	163.0775	0.709	0.332
4	40	164.2414	0.713	0.274
5	50	167.2265	1.817	0.239

Table 2 Heat source at the bottom end of the cavity $M_1 = 1$, $M_2 = 31$ and $N = 51$ ($A = 12$, $\varepsilon = 0.45$, $h = 5$ W/m^2 K, $k = 0.25$ W/m K)

S. no.	M	T_{max} (°C)	Percentage change (abs.)	Discrepancy in energy balance (%)
1	71	165.7752	–	0.126
2	81	164.4237	0.815	0.242
3	91	163.8133	0.371	0.298
4	101	163.4029	0.25	0.323
5	111	163.0775	0.199	0.332
6	121	162.7998	0.17	0.331

Table 3 Heat source at the bottom end of the cavity $M_1 = 1$, $M_2 = 31$ and $M = 111$ ($A = 12$, $\varepsilon = 0.45$, $h = 5$ W/m^2 K, $k = 0.25$ W/m K)

S. no.	N	T_{max} (°C)	Percentage change (abs.)	Discrepancy in energy balance (%)
1	11	162.7159	–	0.479
2	21	162.9234	0.128	0.424
3	31	163.0057	0.082	0.379
4	41	163.0499	0.027	0.351
5	51	163.0775	0.017	0.332
6	61	163.0963	0.012	0.318

N with $M = 111$ and $M_1 = 41$. The results showed that, for this position of the heat source, the optimum values of M_1, M and N, respectively, are 41, 111 and 21.

The third stage of grid study has the heat source at the central position along the left leg of the cavity. For the same set of input parameters as above results are obtained for varying values of M_1 (number of grids in the starting length of the heat source), with $(M_2 - M_1)$ fixed at 30. The optimum value of M_1 is again found to be 41. Subsequently, results with varying values of M and varying values of N indicated the corresponding optimum values to be 111 and 21, respectively. When the heat source takes position between the central and topmost positions, the optimum value of M_1 is found to be 51. For the topmost position of the heat source along the cavity, the values of M_1 and N turned out to be 81 and 31, respectively.

In conclusion to the above studies, the values of M, N and $(M_2 - M_1)$ are globally fixed to be 111, 31 and 30, respectively. However, the value of M_1 for the five chosen positions of the heat source (explained as above) are fixed to be 1, 41, 41, 51 and 81, in that order.

4.2 Validation

In addition to the grid independence and energy balance studies made as above to check the results of the computer code specifically written for solving the present problem, an asymptotic validation too has been made with the results of Dehghan and Behnia [5]. It is to be noted that the work pertaining to the above reference considers combined natural convection–conduction and radiation from the geometry of a discretely heated open cavity with adiabatic bottom boundary. The present problem, on the other hand, considers convection in the entire free to forced convection regime together with conduction and surface radiation. Further, the geometry of the present work has a conducting–convecting–radiating bottom boundary, though, however, the exterior surfaces of all the three solid boundaries are adiabatic here too. In view of this, results from the present code are obtained for the asymptotic free convection limit (Rayleigh number $\approx 3 \times 10^4$) and are subsequently compared with the above reference. A decent agreement within a maximum discrepancy of ±2.41% is noticed between the peak temperature from the present code and that from the above reference. This serves to validate the present results.

4.3 Local wall temperature profiles for different heat source positions

In order to study the nature of temperature variation along the left and right walls of the cavity for different positions of the heat source, results are obtained for $q_v = 10^6$ W/m^3, $A = 12$, $k = 0.25$ W/m K, $h = 5$ W/m^2 K and $\varepsilon = 0.45$. Three different positions of the heat source, namely bottommost, central and topmost, are chosen. A total of six curves are obtained as shown in Fig. 3a, b. The curves of Fig. 3a pertain to the left wall of the cavity and those of Fig. 3b belong to the right wall of the cavity. The notations a, b and c indicate the bottommost, central and the topmost positions of the heat source along the left wall of the cavity. For the bottommost position of the heat source, the local temperature along the left leg initially increases steeply, reaches a maximum, somewhere near the centre of the heat source, and undergoes a steep decrease approximately up to the end of the heat source. Beyond the heat source, the temperature undergoes a nominal decrease up to the central position of the left leg. From this point, the left leg temperature again starts increasing till it reaches a position somewhere beyond the three-quarter length of the left leg, where it assumes a local maximum value. From this position, again the temperature begins to decrease till the top end of the cavity. With regard to the temperature along the right leg, for the same bottommost position of the heat source (in the left leg), the figure shows an initial decrease in temperature as one moves from the bottom of the right leg. However, the right leg temperature starts increasing in

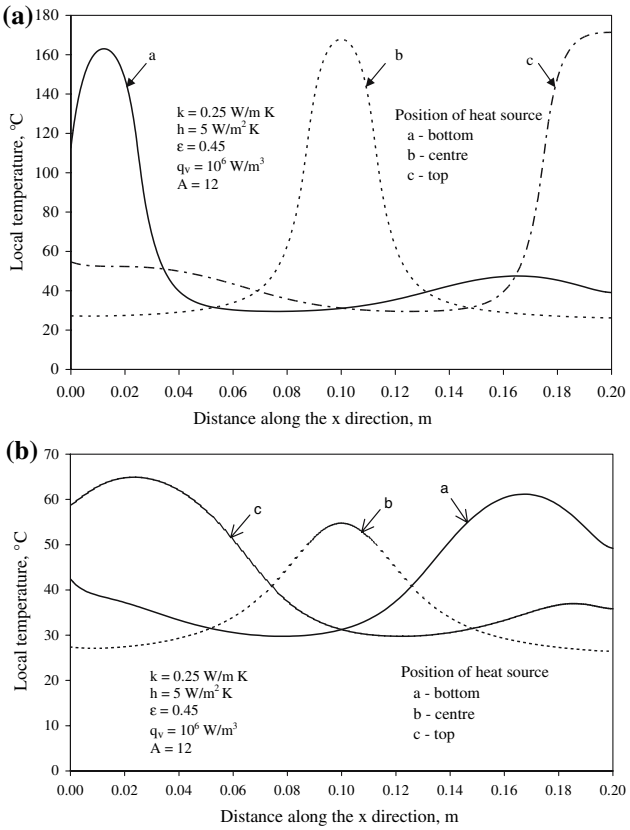

Fig. 3 Variation of local temperature distribution along the **a** left and **b** right legs of the cavity for different positions of heat source

the second-half and reaches a local maximum exactly at the same position where the left leg showed a second local maximum. It may be seen that the local maximum of the right leg is greater than the second local maximum of the left leg. The reason for the increase in the left leg temperature in the second-half is because of the enhanced rate of irradiation coming from the right leg and impinging on the left leg. This is far greater than the sum of the rate of convection heat transfer and emissive power from the left leg over this particular portion of it.

When the heat source is positioned at the centre of the left leg, the local left and right leg temperature profiles, as can be seen in the same figure (Fig. 3), show a perfect symmetry with reference to the centre of each of the legs. As the heat source takes the topmost position of the left leg, the peak temperature (T_{max}) occurs at the top adiabatic end of the leg, which is quite expected. The temperature along the right leg shows exactly the reverse trend in comparison to the case where the heat source is at the bottom end of the left leg.

4.4 Variation of local temperature with other parameters

Figure 4 shows the local temperature distribution along the left leg of the cavity for different surface emissivities. Here the heat source is positioned at the centre of the left leg and results are obtained for $q_v = 10^6$ W/m^3, $A = 12$, $k = 0.25$ W/m K and $h = 5$ W/m^2 K. Three different surface emissivities (ε) are chosen, viz., $\varepsilon = 0.05$, 0.45 and 0.85. The figure shows that an increase in surface emissivity brings down the local temperature in the central portion of the left leg that is spread between 6.5 and 13 cm from the bottom end of the cavity. However, in the initial and final portions of the left leg, each spanning about 6.5 cm in length, the trend is different. Here the temperature profiles cross each other, possibly owing to changes in irradiation and emissive power of the two legs. For example, in the case considered in Fig. 4, the local maximum temperature of the left leg is coming down by 27.96% as ε increases from 0.05 to 0.45. A further increase in ε to 0.85 is bringing down the temperature by about 15.46%. This observation reveals that there is a more pronounced drop in temperature between $\varepsilon = 0.05$ and 0.45 as compared to that between 0.45 and 0.85.

A family of five curves depicting the local temperature profiles along the left leg for five different values of h (5, 10, 25, 50 and 100 W/m^2 K) is drawn as shown in Fig. 5. Here $h = 5$ W/m^2 K signifies the asymptotic limit of free convection, whereas $h = 100$ W/m^2 K signifies the asymptotic forced convection limit. The curves are drawn for a fixed set of parameters, namely $q_v = 10^6$ W/m^3, $A = 12$, $\varepsilon = 0.45$ and $k = 0.25$ W/m K. The figure shows a decrease in the local temperature as the flow regime transits from free to forced convection. However, the degree of decrease in temperature is quite large between $h = 5$ W/m^2 K and $h = 25$ W/m^2 K. The effect of h diminishes as one increases h beyond 25 W/m^2 K. For example, in the present case, the maximum left leg temperature comes down by 54.23% as h rises to 25 W/m^2 K from 5 W/m^2 K. With a further increase in h from 25 to 100 W/m^2 K, the above temperature drops down only by a further 48.45%.

In order to study the effect of thermal conductivity of the cavity on temperature distribution along the left leg possessing the heat source, Fig. 6 has been drawn for $q_v = 10^6$ W/m^3, $A = 12$, $\varepsilon = 0.45$ and $h = 5$ W/m^2 K. Four different values of thermal conductivity, namely $k = 0.25$, 0.5, 0.75 and 1 W/m K, are chosen for the study. The figure shows that, over the portion that contains the discrete heat source, the local leg temperature decreases expectedly

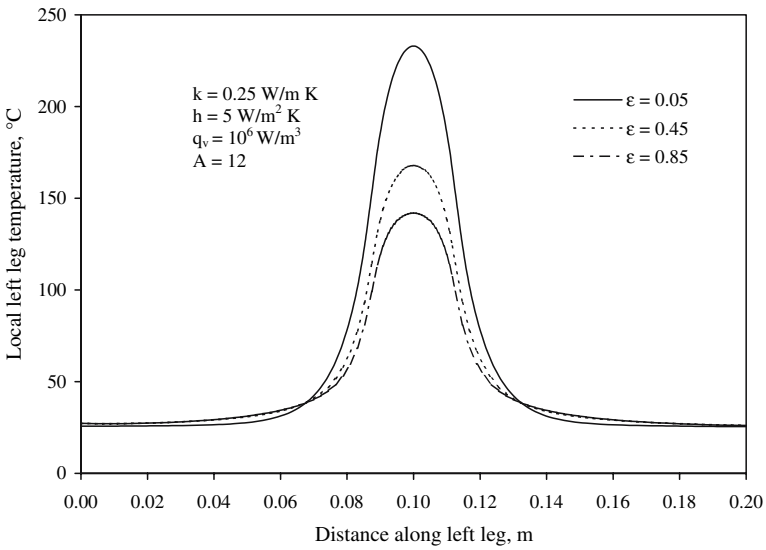

Fig. 4 Local left leg temperature profiles for different surface emissivities

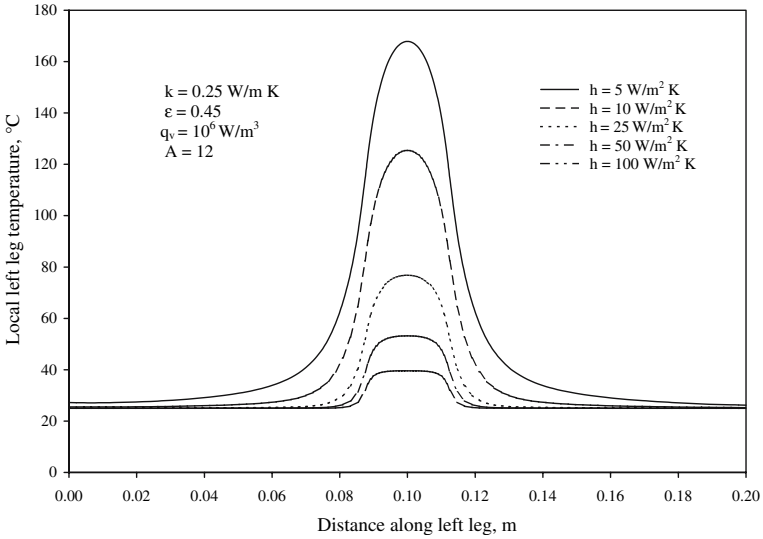

Fig. 5 Variation of local left leg temperature with convection heat transfer coefficient

with increasing thermal conductivity. However, the four curves pertaining to the four values of thermal conductivity chosen are crossing each other at the interfaces between the heat source and the left leg. The curves are, however, almost merging to a temperature equal to the ambient temperature as one goes towards the bottom and top ends of the leg. This reveals that in the case of the cavity with centrally located heat source in the left leg, the role of thermal conductivity is limited only within and the immediate vicinity of the heat source. To quantify, in the heat source portion, in the present example, the maximum left leg temperature is dropping down from 167.85 to 136.72°C as k increases from 0.25 to 1 W/m K.

4.5 Variation of maximum temperature of the cavity with other parameters

Since a control of the peak (or maximum) temperature (T_{max}) that the cavity assumes ensures an effective thermal control of the equipment as a whole, the present section attempts to look into its intricacies.

Figure 7 narrates the variation of maximum left leg temperature with surface emissivity (ε) in different regimes of convection heat transfer. Five different values of ε (0.05, 0.25, 0.45, 0.65 and 0.85) and four different values of h (5, 10, 25 and 100 W/m^2 K) are tried, keeping the remaining parameters, viz., $q_v = 10^6$ W/m^3, $A = 12$ and $k = 0.25$ W/m K, fixed. It is to be noted that $h = 100$ W/m^2 K here is only an asymptotic limiting case for forced convection, which could be reached with air (or any other gaseous medium) as the cooling agent. The figure shows that, in the regime of free convection dominance ($h = 5$ W/m^2 K), T_{max} undergoes a marked drop in its value as ε increases from 0.05 to 0.85. Though this trend of decreasing T_{max} with increasing ε continues in all regimes of convection, the degree of decrement diminishes towards forced convection dominant regime ($h = 100$ W/m^2 K). For example, in the example here, for $h = 5$ W/m^2 K, T_{max} is dropping

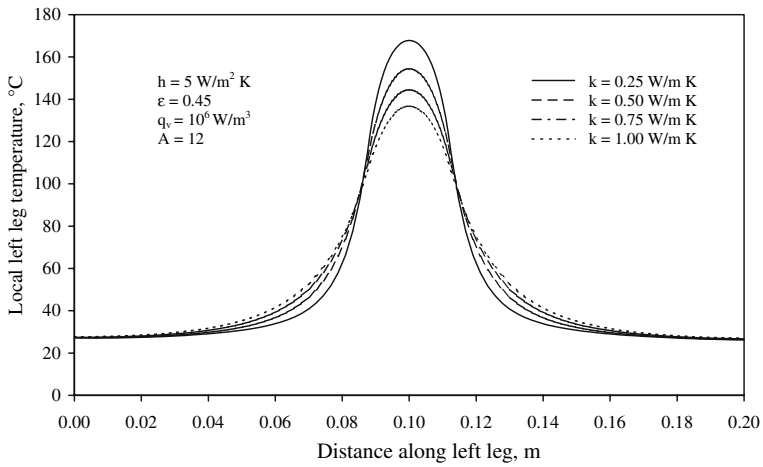

Fig. 6 Local left leg temperature profiles for different thermal conductivities

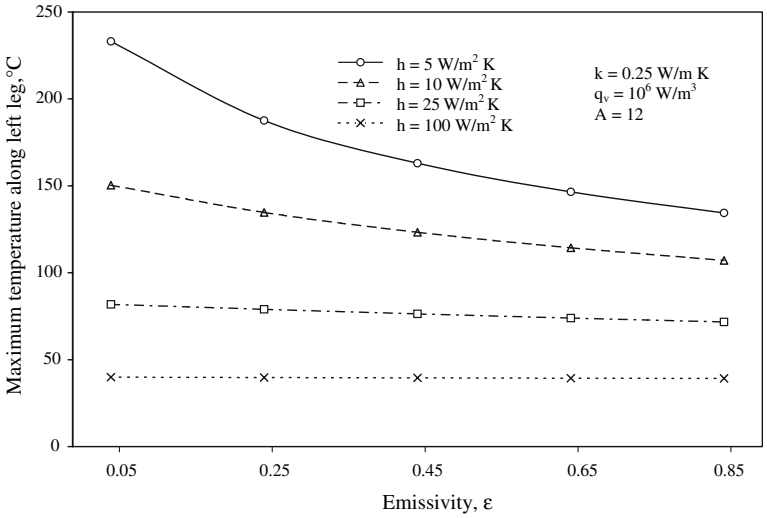

Fig. 7 Variation of maximum left leg temperature with surface emissivity in different regimes of convection

down by as much as 42.34% as ε shoots up from 0.05 to 0.85. In contrast to the above, for $h = 100$ W/m^2 K, T_{max} is decreasing only by 1.81% between the same limits of ε.

To look into the role the aspect ratio (A) plays in the present problem, Fig. 8a, b are drawn. Figure 8a shows the variation of maximum left wall temperature with aspect ratio for different values of surface emissivity, while Fig. 8b shows the same pertaining to the right leg. The study is performed for $q_v = 10^6$ W/m^3, $h = 5$ W/m^2 K and $k = 0.25$ W/m K. Five different aspect ratios, namely 4, 8, 12, 16 and 20, are selected, and three different emissivities 0.05, 0.45 and 0.85 are chosen. Figure 8a indicates that the maximum left leg temperature undergoes a very mild increase as A raises from 4 to 20. It is to be noted that an increasing value of A implies a narrower cavity. In contrast

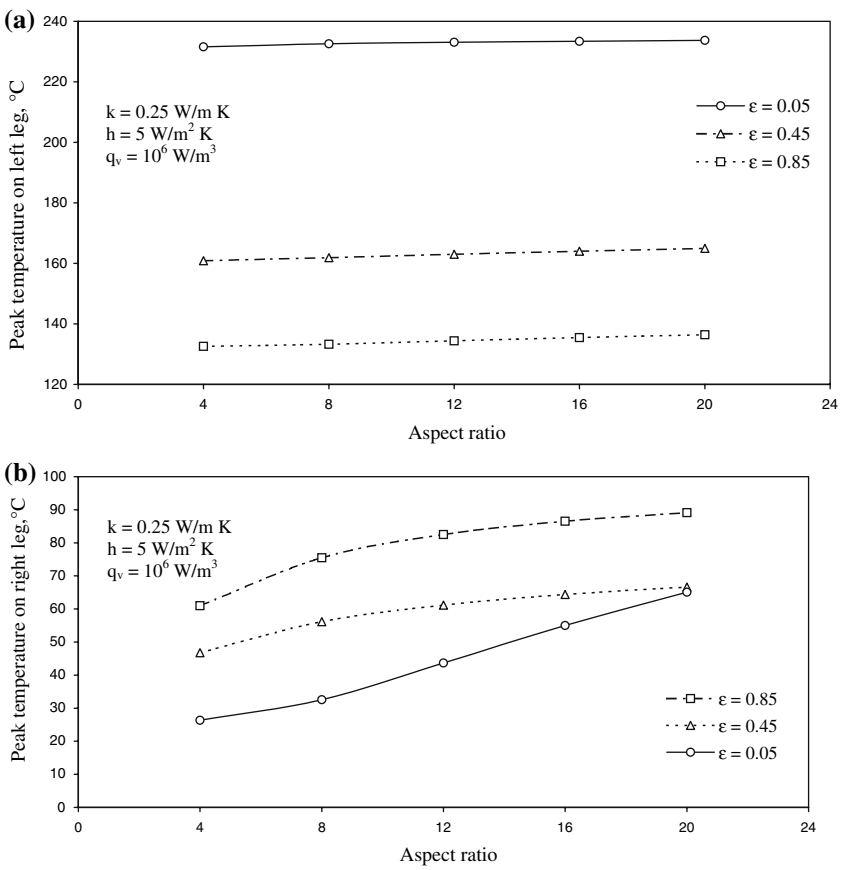

Fig. 8 Variation of maximum **a** left and **b** right leg temperatures with aspect ratio for different surface emissivities

to the above, the peak temperature of the right leg of the cavity shows a considerable increase with increasing aspect ratio for all values of ε. For example, in the case considered here, as A increases from 4 to 20, T_{max} of the left leg increases only by 0.91% for $\varepsilon = 0.05$ and by 2.81% for $\varepsilon = 0.85$. However, in the same range of A, T_{max} of right leg increases by as much as 59.51% for $\varepsilon = 0.05$ and by 31.54% for $\varepsilon = 0.85$.

Figure 9a, b describe the variations of T_{max} of the left and right walls of the cavity, respectively, with aspect ratio for the case where the discrete heat source is positioned at the bottom end of the left leg of the cavity. These figures are plotted for $q_v = 10^6$ W/m^3, $\varepsilon = 0.45$ and $k = 0.25$ W/m K. The entire regime of convection encompassing four values of h (5, 10, 25 and 100 W/m^2 K) is considered. Like in Fig. 8a, here also the aspect ratio (A) shows a nominal effect on T_{max} of the left leg. The above may be noticed from Fig. 9a. For example, with $h = 5$ W/m^2 K, T_{max} of the left leg increases only by 2.53% as A increases from 4 to 20. Figure 9b, similar to Fig. 8b, shows a considerable effect of A on T_{max} of right leg, though only towards smaller values of h, i.e., $h = 5$ and 10 W/m^2 K. In forced convection dominant regime, the effect of A diminishes again. In the case considered here, for $h = 5$ W/m^2 K, T_{max} of right leg increases by 42.36% as A increases from 4 to 20. In the same range of aspect ratio, however, the figure reveals a mild increase of only 0.34% in the peak right leg temperature for $h = 100$ W/m^2 K.

4.6 Relative contributions of convection and radiation to heat dissipation

Since the heat generated in the discrete heat source present in the left leg of the cavity is given to the cooling medium (air) by convection and radiation, it would be interesting to see the role played by each of the above two modes of heat transfer. Figure 10 is plotted depicting the variation of the relative contributions of convection and radiation with surface emissivity (ε) in different regimes of convection. The plot pertains to $q_v = 10^6$ W/m^3, $A = 0.5$ and $k = 0.25$ W/m K and the heat source is located centrally in the left leg. In the figure, the labels 1 and 2 represent the contributions of convection and radiation, while a, b and c correspond to $h = 5$, 10 and 25 W/m^2 K. As can be seen from the figure, convection is the dominant partner for all values of ε in forced convection dominant regime. When

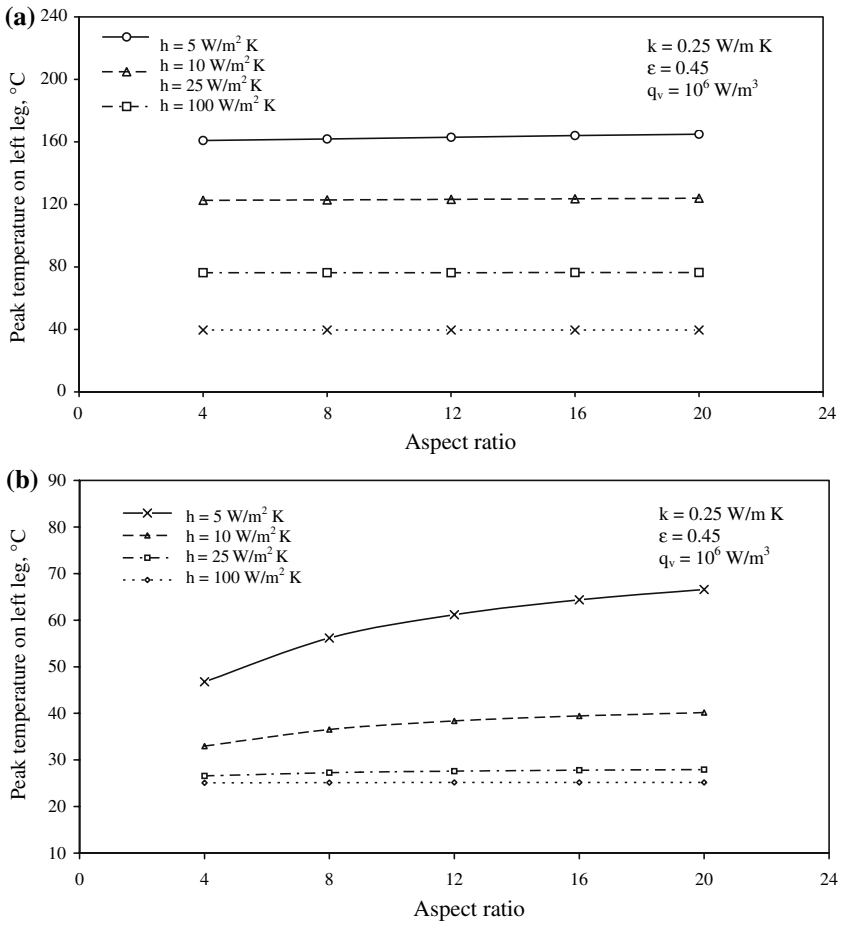

Fig. 9 Variation of maximum left and right leg temperatures with aspect ratio in different regimes of convection

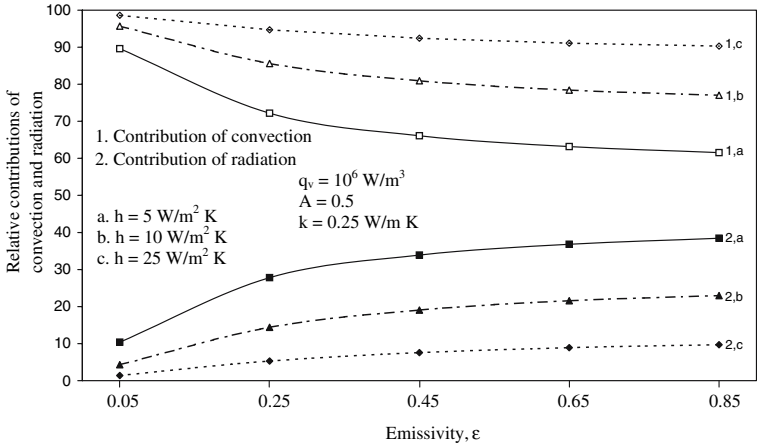

Fig. 10 Relative contributions of convection and radiation with surface emissivity in different regimes of convection

once the flow regime transits to free convection, radiation starts showing an improved effect on heat dissipation in the cavity. This point is substantiated from the curve (2, a) of the above figure, which pertains to $h = 5$ W/m^2 K. Here the contribution of radiation increases from 10.42 to 38.45% as one changes the surface coating of the cavity from a poor emitter ($\varepsilon = 0.05$) to a good emitter ($\varepsilon = 0.85$). This study underlines the importance of radiation in problems of this class, specifically if one is working in the regime of free convection. Even for $h = 10$ W/m^2 K, the role of radiation is considerable enough and it picks up as much as 23% of heat when the cavity is coated with black paint of $\varepsilon = 0.85$.

5 Concluding remarks

The problem of conjugate convection with surface radiation from an open cavity provided with a flush-mounted discrete heat source in its left wall is solved here numerically. The effects of surface emissivity, convection heat transfer coefficient, thermal conductivity and aspect ratio on the results pertaining to the above problem are studied. The best possible position for the discrete heat source has been identified to be the bottom end of the cavity. The fact that the design calculations of the cooling system for problems of this kind should not ignore radiation is substantiated. The point that larger aspect ratios, implying long and narrower cavities are unadvisable is brought out. Further, some sort of optimum values for surface emissivity and convection heat transfer coefficient are proposed.

References

1. Zinnes AE (1970) The coupling of conduction with laminar natural convection from a vertical flat plate with arbitrary surface heating. ASME J Heat Transf 92:528–534
2. Anand NK, Kim SH, Aung W (1990) Effect of wall conduction on the free convection between asymmetrically heated vertical plates: uniform wall temperature. Int J Heat Mass Transf 33:1025–1028
3. Tewari SS, Jaluria Y (1990) Mixed convection heat transfer from thermal sources mounted on horizontal and vertical surfaces. ASME J Heat Transf 112:975–987
4. Merkin JH, Pop I (1996) Conjugate free convection on a vertical surface. Int J Heat Mass Transf 39:1527–1534
5. Dehghan AA, Behnia M (1996) Combined natural convection-conduction and radiation heat transfer in a discretely heated open cavity. ASME J Heat Transf 118:56–64
6. Cole KD (1997) Conjugate heat transfer from a small heated strip. Int J Heat Mass Transf 40:2709–2719
7. Gururaja Rao C, Balaji C, Venkateshan SP (2001) Conjugate mixed convection with surface radiation from a vertical plate with a discrete heat source. ASME J Heat Transf 123:698–702
8. Gururaja Rao C, Balaji C, Venkateshan SP (2003) Conjugate mixed convection with surface radiation in a vertical channel with symmetric and uniform wall heat generation. Int J Transp Phenomena 5:75–101
9. Gururaja Rao C, Balaji C, Venkateshan SP (2002) Effect of surface radiation on conjugate mixed convection in a vertical channel with a discrete heat source in each wall. Int J Heat Mass Transf 45:3331–3347
10. Gururaja Rao C (2004) Buoyancy-aided mixed convection with conduction and surface radiation from a vertical electronic board with a traversable discrete heat source. Numer Heat Transf Part A 45:935–956
11. Gururaja Rao C, Venkata Krishna A, Naga Srinivas P (2005) Simulation studies on multimode heat transfer from a square-shaped electronic device with multiple discrete heat sources. Numer Heat Transf Part A 48:427–446